

## Study on Dynamic Compressive Mechanical Properties and Failure Modes of Heat-Treated Granite

### Abstract

Temperature and external load are two important factors affecting the mechanical properties of rock material. The test on heat-treated granite specimen was carried out by using an improved split Hopkinson pressure bar (SHPB). Based on the test data, the dynamic behavior and failure characteristics of the granite under the coupling action of temperature and impact loading are studied. The results show that the amplitude of incident wave increases with the impact velocity of striker, and the shapes of the transmitted and reflected waves are closely related to the failure state of the specimen. The stress-strain curves for the heat-treated specimens above 700°C are obviously different to those below 500°C in terms of the slopes for the ascending segment and the peak stress, indicating that there is a temperature threshold between 500°C and 700°C. Under the same velocity, the strain rate decreases slightly and then increases as the temperature increases. At a constant temperature, strain rate increases linearly with the impact velocity. The relationship between elastic modulus and strain rate for the heat-treated specimen obviously tends to have no regularity. In addition, both peak stress and peak strain exhibit strain rate sensitivity, but different increasing rates for different temperatures are detected. Below 500°C, the influence of temperature on peak stress and peak strain is not evident, however, the influence becomes remarkable at 700°C and 900°C.

### Keywords

Granite; Temperature; SHPB test; Mechanical property; Failure mode; Strain rate

Zhiliang Wang \*

Shiyun Hao

School of Civil & Hydraulic Engineering,  
Hefei University of Technology, Hefei,  
230009 Anhui Province, China

\* Corresponding author:

[cvewzL@tongji.edu.cn](mailto:cvewzL@tongji.edu.cn)

<http://dx.doi.org/10.1590/1679-78253342>

Received 04.09.2016

In revised form 12.02.2017

Accepted 21.02.2017

Available online 04.03.2017

## 1 INTRODUCTION

Rock dynamics, an important branch of rock mechanics, is a new discipline that deals with mechanics and vibration effect problems such as stress, strain, acceleration, fracturing, damage, etc., under

the action of earthquake, explosion and other dynamic factors. In practice, the circumstances surrounding rock are very complex, with the combined effect of temperature field and dynamic load, such as the exploitation of deep ore deposit, the utilization of geothermal resource, the disposal of high radioactive nuclear waste, the reconstruction of tunnel damaged by fire and so on. Therefore, it is of importance to carry out the study on the dynamic properties of heat-treated rock, and it has great significance to engineering applications.

So far, great achievements have been made in the strain rate effect of rocks: Jackson et al. (2008) conducted the uniaxial compression test on rock with a wide range of strain rate, and concluded that the influence of strain rate on the fracture characteristics of rock was remarkable. Chong et al. (1980) performed dynamic compression tests for oil shale with the strain rate varied between  $10^{-4}/s$  and  $10/s$ , and indicated that the compressive strength increased with the increase of logarithmic strain rate. Qi et al. (2009) pointed out that the deformation and fracture of rock were dominated by the heat-activated mechanism at low strain rate. However, the macroscopic viscosity was found to emerge and gradually prevail with increasing strain rate. The study on mechanical parameters (liang et al., 2015) showed that the elastic modulus increased with the ratio of specimen height to diameter and strain rate, whereas the Poisson's ratio was independent of these two factors. Jeong et al. (2007) stated that the compressive strength exhibited a positive correlation with strain rate, while the stress damage index hardly depended on strain rate. Lu & Wang (2016) explored the dynamic characteristics of granite under medium-high strain rate, and found that the compressive strength increased logarithmically with strain rate, but the elastic modulus was not sensitive to the confining pressure and strain rate. Zhai et al. (2007) used a sliding-type microcrack model to explain the rate-relevance of compressive strength and the dynamic fracturing of rock.

In the field of rock thermomechanics: Yuan et al. (2011) dealt with the existence of time-temperature equivalence, the experiment results showed both elastic modulus and viscosity coefficient of the Burger model decreased with temperature at an exponential rate. Uniaxial compression tests were performed on saltrock by Sheinin et al. (2012), studying the relationship between the nonlinear deformation stage and the thermo-mechanical feature. Rocchi et al. (2002) analyzed the testing data for basaltic rock under high temperature, and then plotted the envelopes of the principal stress direction. Liu et al. (2015) experimentally explored the physical and mechanical properties of granite and sandstone subjected to high temperature, and indicated the effect of temperature on physical property of rocks was more intense than that on mechanical property. Nasser et al. (2009) investigated the interrelationship between the toughness and roughness of fracture for thermally treated granite, and found the phase-transition of quartz in a range of  $450^{\circ}C$  to  $650^{\circ}C$ , causing a large increase of microcracks. Ozguven et al. (2014) studied the physical and mechanical properties of limestone and granite under different temperatures, and pointed out that the tensile strength of rocks decreased with increasing temperature, and the strength became much low for a temperature above  $600^{\circ}C$ . Funatsu et al. (2004) conducted the fracture toughness experiments under  $200^{\circ}C$ . The results showed that when the temperature exceeded  $125^{\circ}C$ , the increase of fracture toughness resulted from the microcrack closure. Zhang et al. (1996) focused on the effect of temperature on the microstructure of quartzite, and reported that the difference in thermal stress of minerals was the chief reason of damage.

Although numerous studies were carried out on mechanical properties of rock, these works were limited primarily to test at room temperature or consideration of thermal effect under static load. It is well-known that the mechanical properties of rock show strong dependence on both temperature and strain rate in many engineering constructions. Therefore, the improved split Hopkinson pressure bar (SHPB) tests on granite specimens are performed in this study, varying the values of treatment temperature and impact velocity (loading rate). Based on the test results, the shape of stress-strain curve, the failure mode of heat-treated specimen, the strain rate effect on elastic modulus along with the variation laws of peak stress and peak strain (strain at the peak stress) are investigated. Some useful conclusions are then given and helpful for the design of rockmass engineering exposed to high temperature.

## 2 EXPERIMENT CONFIGURE

### 2.1 Experimental Material

The granite was taken from the quarry in the Huashan area (Shanxi Province, northwest China). Generally, Huashan granite has a gray and lumpy structure, classified as medium-fine-grained biotite granite. The main mineral compositions include microcline (41%), plagioclase (27%), quartz (22%) and biotite (7%) and others. The average density of granite is  $2620\text{kg/m}^3$ . The rock specimens were first core-drilled from a large granite block. The specimens were then cut from the high-quality cores with an electric cut-off machine. The specimens for the impact compression test have a diameter of 50mm and a length of 25mm to meet the assumption of stress uniformity (Christensen, 1972; Dai et al., 2010). The specimens were carefully ground by a grinding machine to ensure that the parallelism between the top and bottom surface of the specimen is within 0.05mm. The working accuracy of the granite specimens conforms to the standard suggested by the International Society for Rock Mechanics (ISRM).

### 2.2 Specimen Preparation and Testing Principle

In this study, six groups of specimens were prepared including one obtained at room temperature and the other five treated at  $100^\circ\text{C}$ ,  $300^\circ\text{C}$ ,  $500^\circ\text{C}$ ,  $700^\circ\text{C}$ , and  $900^\circ\text{C}$ , respectively. Each group had 9-15 specimens and was tested with three different impact velocities to ensure at least three effective data for each case. The thermal treatment was conducted in a servo-controlled electrical furnace at a rate of  $10^\circ\text{C}/\text{min}$ . As soon as the temperature reached a specified value in the furnace, the temperature was maintained for 4h. Then, the furnace was cooled down to room temperature in a natural state. Figure.1 shows the granite specimens subjected to different temperatures. As an important physical property of rock, the ultrasonic P-wave velocity was measured with the ultrasonic tester before and after the thermal treatment.

As shown in Figure.2a, SHPB consists of elastic incident and transmitted bars with a short specimen sandwiched between them (Figure.2b) (Kolsky, 2002). The impact of the striker at the free end of the incident bar motivates a compressive longitudinal incident wave  $\varepsilon_i(t)$ . Once this wave arrives at the interface between the incident bar and the specimen, a part of it,  $\varepsilon_r(t)$ , is reflected, whereas another part  $\varepsilon_t(t)$  passes through the specimen and transmits to the transmitted

bar. Those three basic waves are recorded by the gauges mounted on the incident and transmitted bars.

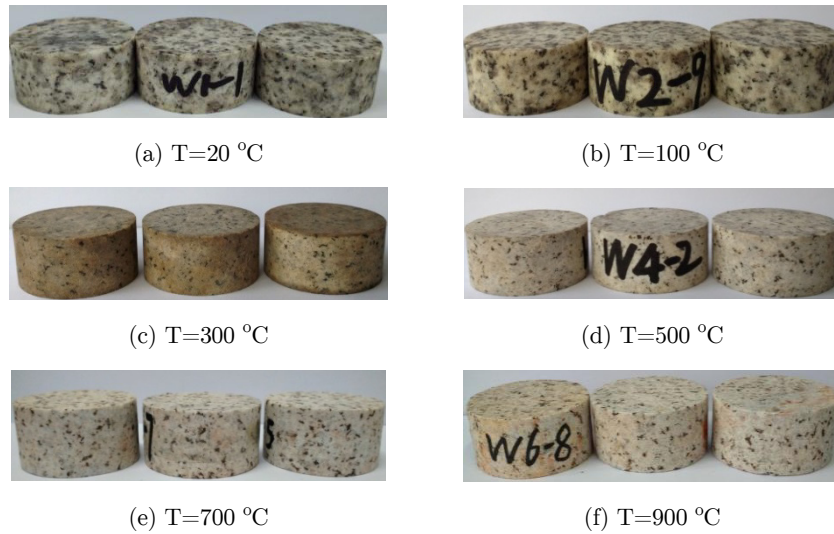


**Figure 1:** Granite specimens after different treatment temperatures.

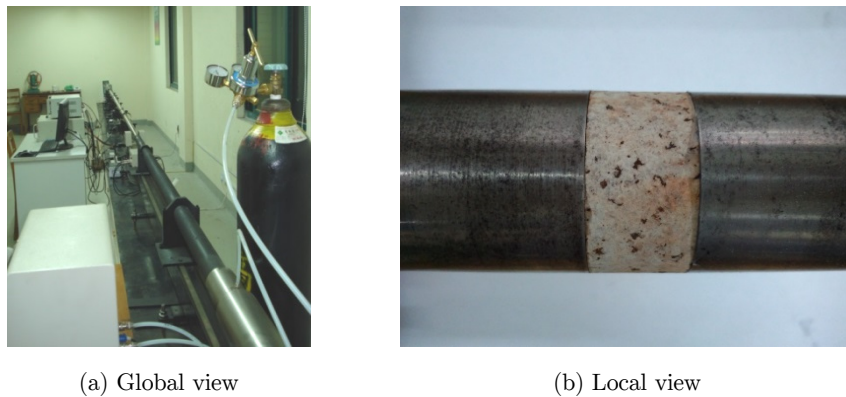


**Figure 2:** Photos of split Hopkinson pressure bar.

According to the wave propagation theory and two basic assumptions (Wu, et al., 2010), the average stress, strain and strain rate of the specimen can be calculated by the following equations (Zhou, et al., 2012):

$$\sigma(t) = \frac{A}{2A_s} E(\varepsilon_i(t) + \varepsilon_r(t) + \varepsilon_t(t)) \tag{1}$$

$$\varepsilon(t) = \frac{c}{l_s} \int_0^t (\varepsilon_i(t) - \varepsilon_r(t) - \varepsilon_t(t)) dt \tag{2}$$

$$\dot{\varepsilon}(t) = \frac{c}{l_s} (\varepsilon_i(t) - \varepsilon_r(t) - \varepsilon_t(t)) \quad (3)$$

where  $A$  and  $A_s$  are the cross-sectional areas of bars and specimen, respectively;  $E$  is the elastic modulus of the bars;  $c$  and  $l_s$  are the wave velocity in bars and the original length of specimen, respectively.

For the SHPB system used in this study, the lengths of the striker bar, incident bar, and transmitted bar are 400, 1400, and 1000 mm, respectively. The wave velocity of the bars is 5172m/s and the elastic modulus is 210GPa. In SHPB tests, the impact velocity is mainly controlled by changing the pressure of compressed gas, so the amplitude of strain-rate is changed. Under each temperature level, three loading gas pressures (0.22MPa, 0.32MPa and 0.48MPa) were selected, thus the SHPB tests on the granite specimens have been conducted under 3 kinds of average velocities (11.0m/s, 14.5m/s and 19.0m/s). To reduce the end friction effect, vaseline was smeared on the interfaces between specimen ends and incident bar or transmission bar.

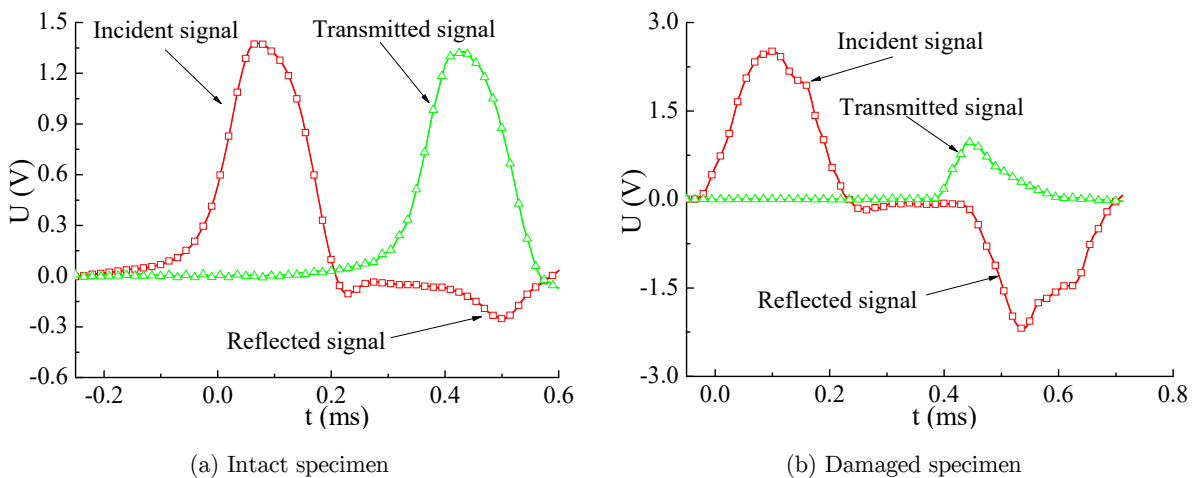


Figure 3: Comparison of incident and transmitted wave signals.

To ensure that uniform stress state in the loading direction can be achieved early in specimens and that the amplitude of pulse oscillation can be reduced, soft rubber with the diameter of 10.0 mm and the thickness of 3.0 mm was employed as pulse shaper through multiple trial tests (Frew, Forrester & Chen., 2002). The original stress wave curves are shown in Figure 3. It can be seen that the incident wave has a shape similar to a bell-like waveform with a smoother and longer ramp, especially suitable for dynamic loading of brittle material. Additionally, the transmitted wave is very weak while the reflected wave accordingly becomes strong for a damage specimen.

### 3 EXPERIMENT RESULTS AND DISCUSSION

Strength and deformation of rock are important consideration for the design and stability analysis of slope engineering and the underground cavern. Both the two aspects may be characterized by peak stress, peak strain, strain rate, elastic modulus and so on, most of which can be extracted from

the complete stress-strain curves of rock. Therefore, the coupling effect of temperature and dynamic load on mechanical properties and failure modes of heat-treated granite will be discussed below by taking these indexes as a starting point.

### 3.1 Waveform Curve and Failure Mode of Specimen

Figure.4 presents the recorded waveform at room temperature. It is clear that under different impact velocities, the shapes of the incident waves are similar, and the amplitude of incident wave increases as the impact velocity increases. However, the damage status of specimens has a great influence on transmitted waves. For impact velocities of 11.0m/s and 14.5m/s, the specimen damage is relatively mild (Figure.5). The amplitude of transmitted wave is about 90% of the incident wave, while the reflected wave is obviously lower. As the impact velocity rises to 19.0m/s, serious failure of the specimen occurs (Figure.5c) and thus the effective contact area between the specimen and the bars decreases rapidly, resulting in the attenuation of transmitted wave. Accordingly, a relative increase in reflected wave was detected. As shown in Figure.5, the specimens are almost intact at lower impact velocity and room temperature. With the increase of velocity, cracking starts from the outer edge of the specimens, followed by the fracturing. After high-velocity impact, the specimens are broken into small pieces.

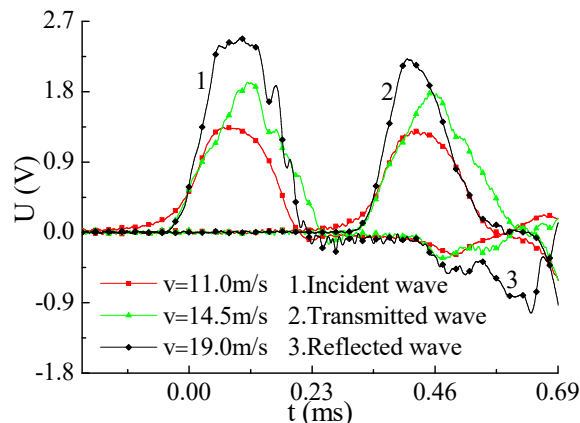


**Figure 4:** Waveform curves under different velocities at room temperature.

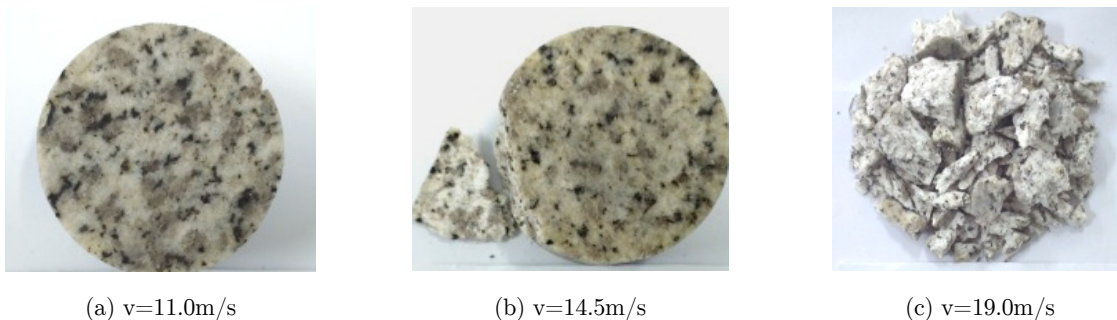


**Figure 5:** Failure modes of specimens under different velocities at room temperature.



Figure.6 shows the typical incident, reflected and transmitted waves shaped by the pulse shaper with an impact velocity of 14.5m/s. The incident waves under different temperatures are almost identical, indicating that the impact velocity and the shaping effect were well regulated. For specimens that are not crushed, a stable transmitted wave was recorded. Otherwise, a significant decrease in the transmitted wave was detected. For example, at the 700°C and 900°C, the amplitudes of transmitted waves decrease rapidly, while those of reflected waves rise correspondingly. It may be inferred that there exists a temperature threshold between 500°C and 700°C. When the temperature is below 500°C, the damage of specimen at the impact velocity of 14.5m/s is relatively mild (Figure.7). The damage of specimen generally becomes more serious as the temperature increases, with the specimen pulverizing at 900°C.

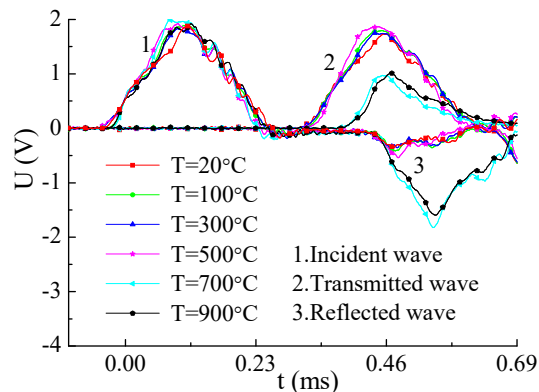


Figure 6: Waveform curves under different treatment temperatures at  $v=14.5\text{m/s}$ .

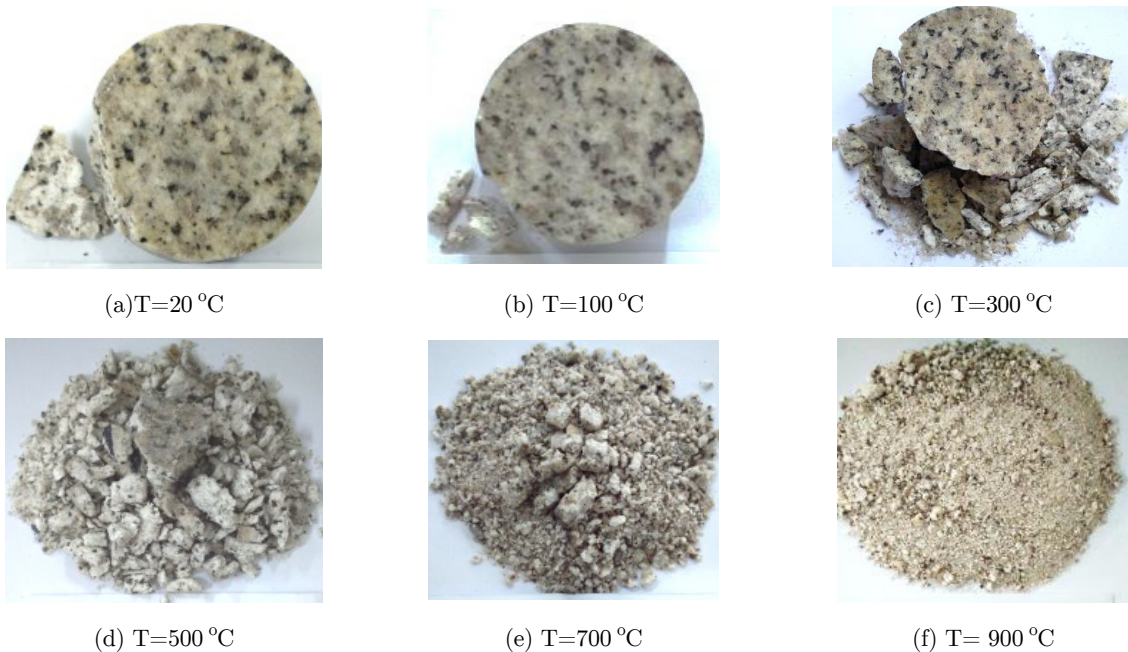


Figure 7: Failure modes of specimens under different temperatures at  $v=14.5\text{m/s}$ .

### 3.2 Shape of Stress-Strain Curve

The SHPB tests on the granite specimens were conducted at three impact velocities and six temperatures. The stress-strain curves obtained from the SHPB tests are plotted in Figures.8 and 9. These curves were calculated from the strain signals recorded in the bars using Eqs.(1)-(3). The dynamic strength is defined as the peak stress herein.

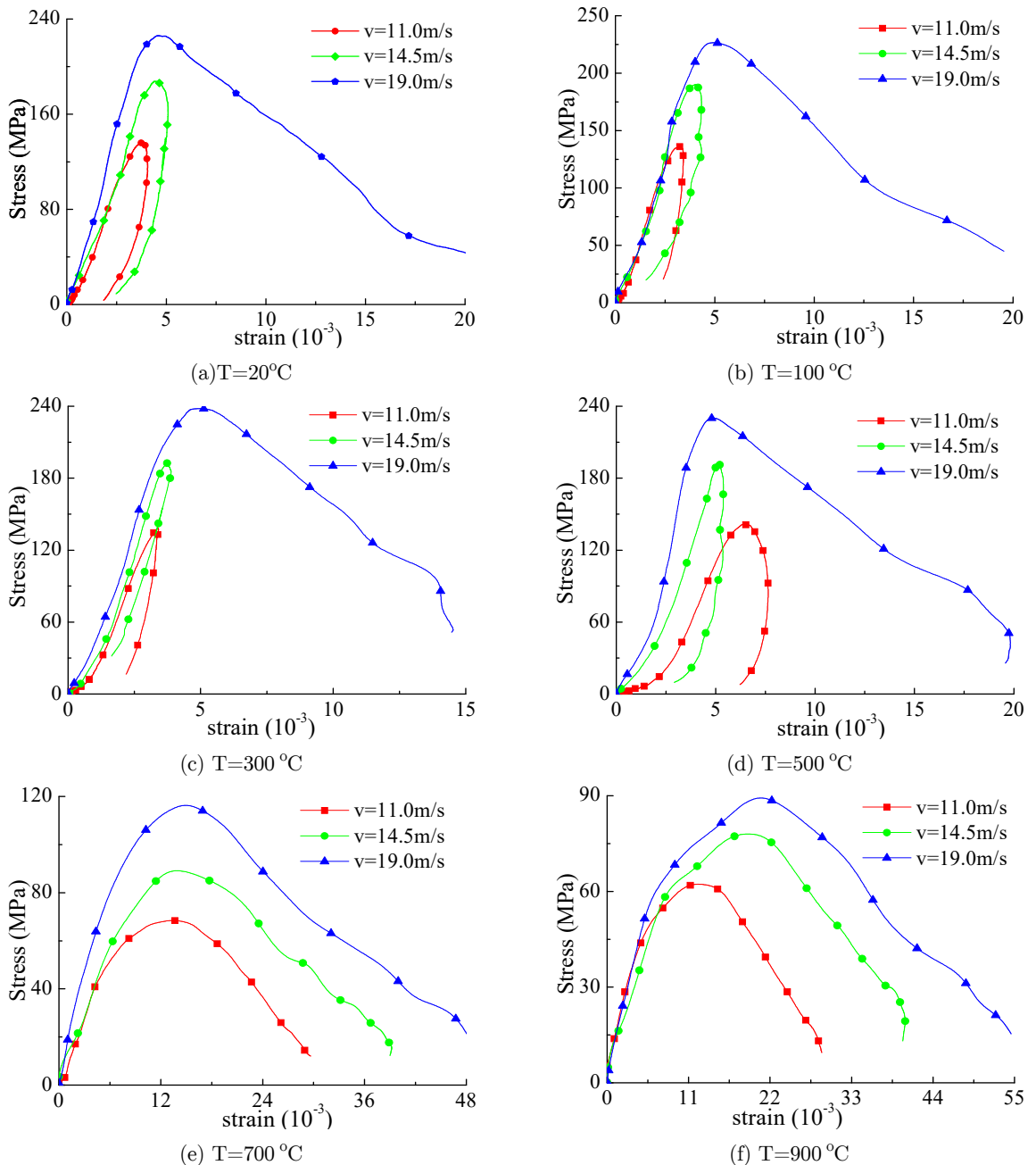


Figure 8: Stress-strain curves under different impact velocities.



According to Figure.8, the stress increases linearly initially and then decreases after the stress achieves the peak value. The rebound phenomenon can be noticed for the impact velocities of 11.0m/s and 14.5m/s. As the velocity rises up to 19.0m/s, the specimen breaks into pieces and the stress-strain curve manifests the strain-softening behavior. In addition, Figure.8 indicates when the temperature falls below 500°C, the shapes of stress-strain curves are very similar, i.e, the slopes of the ascending segment of stress-strain curves are very close to each other, whereas the descending segment of the curves is considerably affected by the impact velocity. At higher temperatures of 700°C and 900°C, the specimen strength significantly deteriorates due to thermal damage, and there is no rebound phenomenon in stress-strain curves even under low impact velocity. Figure.9 shows the stress-strain curves of specimens subjected to different temperatures. It can be seen that for the temperatures at 500°C and below, the shapes of stress-strain curves are alike. Besides, the slopes of the ascending segment and the peak stress are hardly changed, indicating that the effect of temperature on the compressive strength and elastic modulus is little. As the treatment temperature rises to 700°C or above, the peak stress and elastic modulus decrease significantly, whereas peak strain is mobilized and dramatically increases, which further confirms that there exists a temperature threshold between 500°C-700°C for Huashan granite.

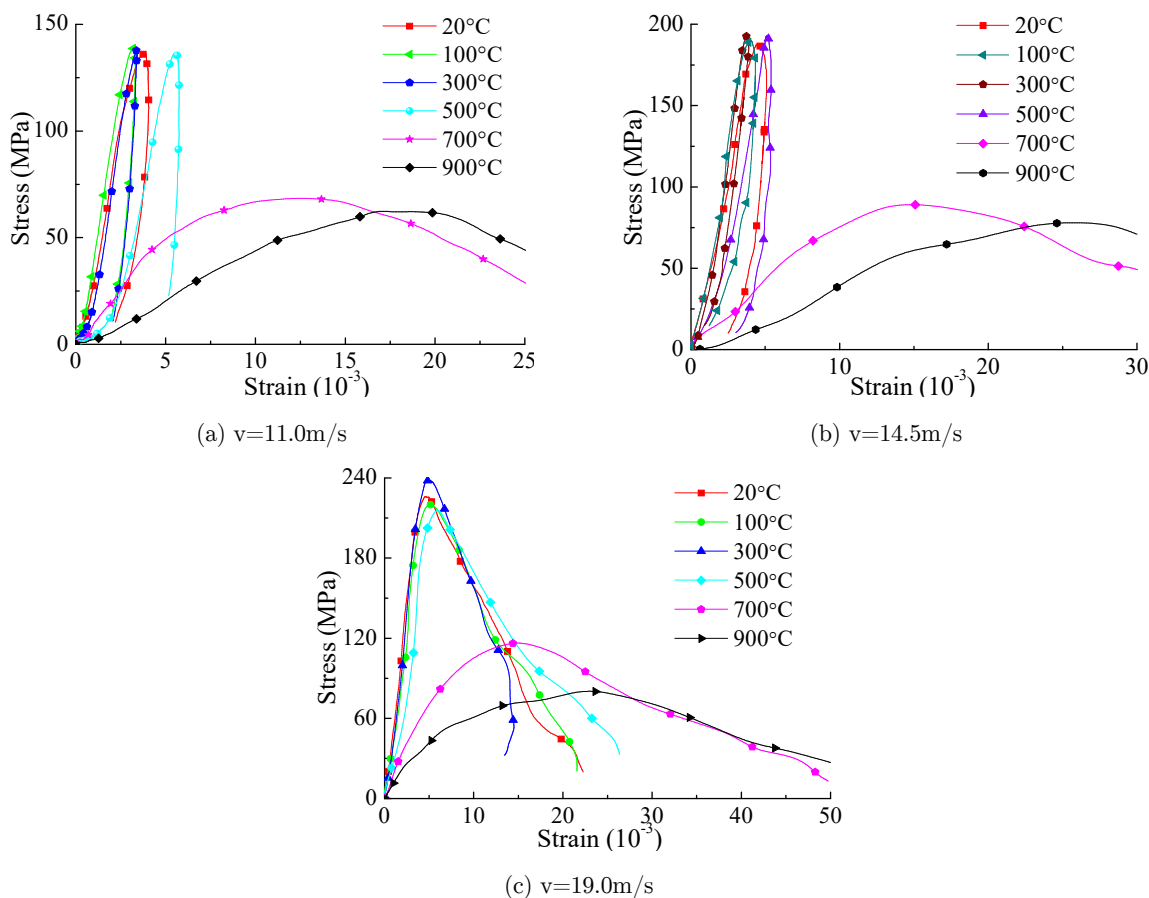


Figure 9: Stress-strain curves under different treatment temperatures.

### 3.3 Influencing Factors of Strain Rate

The effect of treatment temperature and impact velocity on the strain rate is discussed in this section. For convenience, the average strain-rate is adopted in this study, which is defined as the ratio of strain increment to time increment at the peak stress. The variation of average strain rate as a function of temperature for impact velocities of 11.0, 14.5 and 19.0 m/s is shown in Figure.10. It can be seen that under the same impact velocity, the strain rate decreases slightly as the temperature increases from 200°C to 400°C and then increases significantly with increasing temperature above 400°C. The decrease is caused by the volume expansion of mineral grains due to the vaporization of strong bound water, which may make the rock specimen denser.

Figure.11 shows the relationship between strain rate and impact velocity for different temperatures (20°C-900°C). Overall, the strain rate increases linearly with the impact velocity under different temperatures. A good correlation between the impact velocity and strain rate is exhibited. In addition, for a similar impact velocity, the higher the temperature is, the greater the corresponding strain rate is. Especially for the 700°C and 900°C cases, the increasing trend of strain rate is extraordinarily clear, which shows the rate effect still remains at higher temperature.

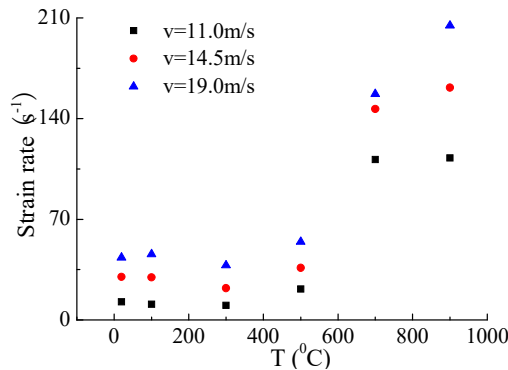


Figure 10: Variation of strain rate and treatment temperature.

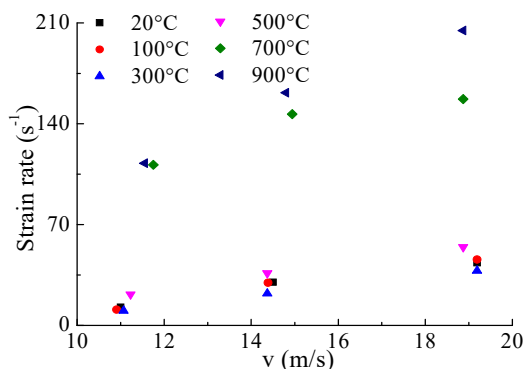


Figure 11: Variation of strain rate and impact velocity.

### 3.4 Characteristics of Elastic Modulus

The elastic modulus is calculated using the equation below (Liu & Xu, 2015):

$$E_c = \frac{\sigma_2 - \sigma_1}{\varepsilon_2 - \varepsilon_1} \tag{4}$$

where  $\sigma_1$  and  $\varepsilon_1$  are, respectively, the stress and strain at the point of which the stress is 40% of the peak stress; and  $\sigma_2$  and  $\varepsilon_2$  are, respectively, the stress and strain at the point of which the stress is 60% of the peak stress.

The relationship between strain rate and elastic modulus is plotted in Figure.12 for different temperatures between 20°C and 900°C. No obvious trend can be observed. For temperatures below 500°C , the dynamic elastic modulus ranges from 40GPa to 60GPa. The value is significantly lower at the temperatures of 700°C and 900°C , and it nearly remains constant with the increase of strain rate. Figure.13 shows the variation of elastic modulus with treatment temperature under impact velocities of 11.0, 14.5 and 19m/s. For the velocity of 14.5m/s, the elastic modulus decreases from 47GPa to 11GPa as the temperature increases from 500°C to 700°C. A further reduction by 45% as the temperature increases from 700°C to 900°C. To further investigate the effect of temperature treatment on the elastic modulus of granite, the relative elastic modulus (ratio of the elastic modulus at a certain temperature to that at room temperature of 20°C ) is shown in Figure.14 (Du, 2004). It is seen that after the thermal treatment with a temperature of 700°C , the elastic modulus of specimen decreases by about 80% compared to the room temperature, suggesting that the specimen has severe thermal damage at that moment.

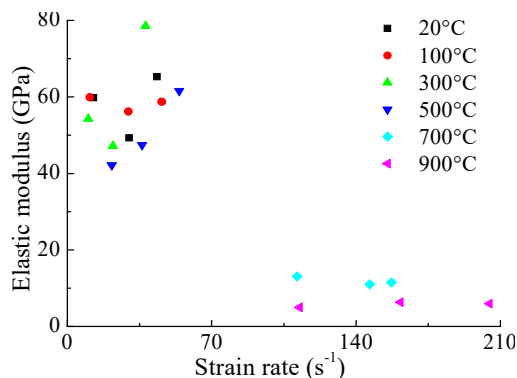


Figure 12: Variation of elastic modulus and strain rate.

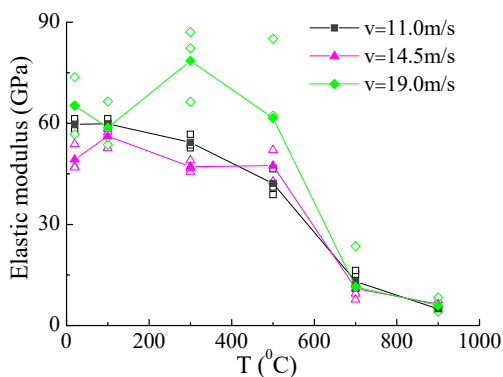


Figure 13: Plot of elastic modulus and treatment temperature.

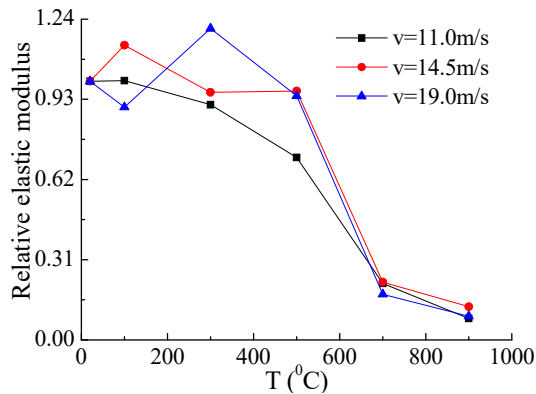


Figure 14: Plot of relative elastic modulus and treatment temperature.

### 3.5 Variation Law of Peak Stress

The magnitude of peak stress is shown in Figure.15 in terms of strain rate. Under different temperatures, the peak stress of specimen increases with increasing strain rate, but the increasing rates (or gradients) are not consistent. For temperatures at and below 500°C, the peak stress increases with the strain rate in a similar way, and the gradient is much steeper compared to those for temperatures of 700°C and 900°C. For example, at 900°C, the gradient of increase is only 0.36, reduced by 87% compared to that at room temperature.

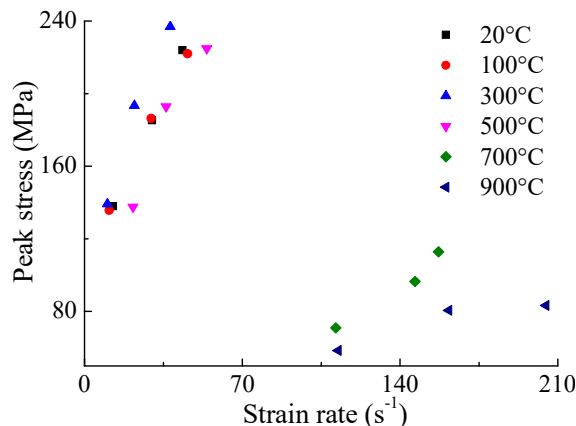


Figure 15: Variation of peak stress and strain rate.

The variation of peak stress with different temperatures is given in Figure.16, declaring that when the temperature falls within 500°C, the change of peak stress with temperature is insignificant. For temperatures above 500°C, the peak stress reduces considerably with increasing temperature. At the velocity of 11.0m/s, the peak stress decreases from 138MPa to 58.5MPa as the temperature increases from 20°C to 900°C. At the same time, it can be seen that the discreteness of the data points of peak stress under three impact velocities abates as the temperature rises, indicating that the average strength of the heat-treated specimen drops as a whole.

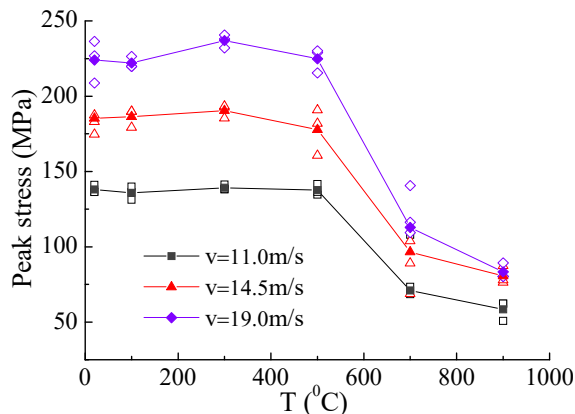


Figure 16: Plot of peak stress and treatment temperature.

The relative peak stress, one of the major indexes, which is taken as the ratio of peak stress of heat-treated specimen to the peak stress at room temperature (Du, 2004), is plotted in Figure.17. For a temperature at or below 500°C, the range of peak stress fluctuates within ±6.0%. Once the temperature reaches 500°C or above, the relative peak stress reduces significantly. For the temperature of 900°C, the average peak stresses of all specimens under different impact velocities reduce by about 60% compared to those at the room temperature. These results imply that the influence of temperature on the granite property is slight under 500°C. When the temperature exceeds 500°C, the loss of mineral combined water and the phase-transition of quartz happen (Branlund, et al., 2007; Yin, et al., 2012), which lead to deterioration of the macroscopic mechanical properties and the significant decrease of granite strength.

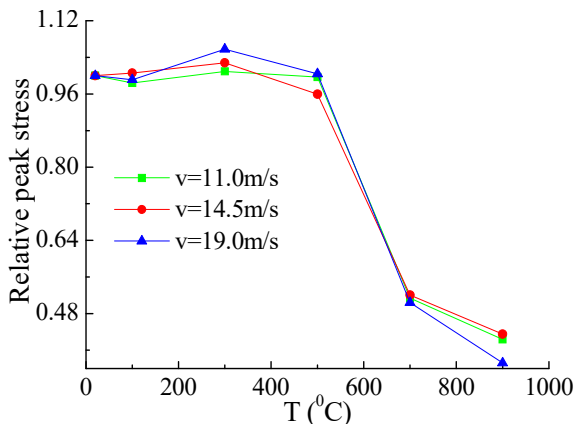


Figure 17: Plot of relative peak stress and treatment temperature.

### 3.6 Variation Law of Peak Strain

Figure.18 shows the relation between peak strain and strain rate for a range of temperatures from 20°C to 900°C. It is observed the peak strain of the specimen increases with increasing strain rate, but the gradients of increase for different temperatures are not consistent. For a range of 100°C to

300°C, the gradient are close to each other, with an average value of about  $4.3 \times 10^{-2}$  ms. At 500°C, the gradient drops to  $5.2 \times 10^{-3}$  ms. For temperatures over 500°C, the gradient continuously increases, and the value reaches 0.14ms at 900°C. The effect of treatment temperature on peak strain is plotted in Figure.19 for impact velocities of 11.0, 14.5 and 19m/s. For a temperature lower than 500°C, the peak strain is hardly affected by the temperature, whereas it increases significantly once the temperature goes beyond 500°C. For example, at an impact velocity of 11.0m/s, the peak strain increases by  $2.81 \times 10^{-3}$  and  $1.81 \times 10^{-2}$  as the temperature increases from 300°C to 500°C and from 500°C to 900°C, respectively. The gradient of the latter is about three times greater than the former.

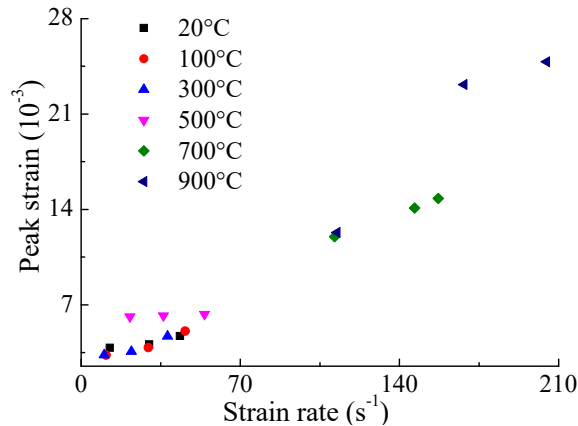


Figure 18: Variation of peak strain and strain rate.

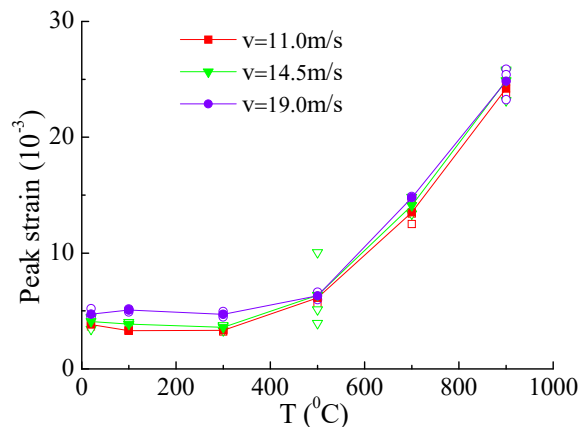


Figure 19: Plot of peak strain and treatment temperature.

Figure.20 presents the value of peak strain relative to that at room temperature. At the temperature of 500°C, the average peak strain of all specimens increases by approximately 49% compared to that at the room temperature. For the 900°C specimen, the average peak strain is about six times greater than that for room temperature. This is due to the dilapidation of crystalline structures. and phase-transition of quartz when the temperature rises, resulting in a larger deformation under the same stress state.

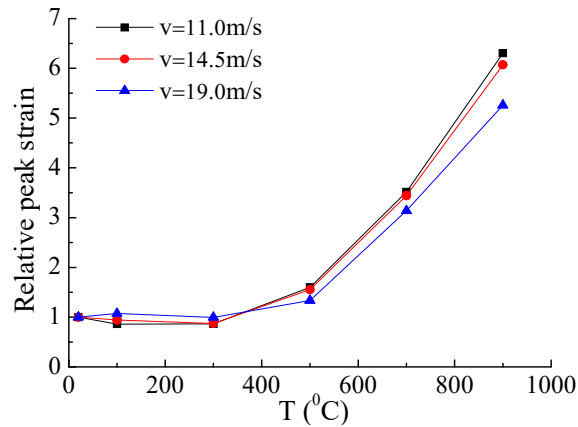


Figure 20: Plot of relative peak strain and treatment temperature.

## 4 CONCLUSIONS

In this work, the impact compression behavior of heat-treated granite was studied. Based on the experimental results and observations, the following main conclusions can be drawn:

(1) The amplitude of incident wave increases in direct proportion to the impact velocity of the striker, and the shapes of the transmitted and reflected waves are related to the failure state of specimen tested. As the damage of the specimen intensifies, the amplitude of transmitted wave reduces while that of reflected wave increases accordingly.

(2) Impact velocity and thermal treatment exert significant influences on the shape of stress-strain curve. For the temperatures at and below 500°C, the ascending segments of the stress-strain curves are almost coincident. Once the temperature reaches 700°C, the peak stress and elastic modulus decreases significantly, implying that there exists a temperature threshold between 500°C and 700°C.

(3) Strain rate falls slightly in the temperature range of 200°C-400°C, and then increases with the treatment temperature for a fixed impact velocity. At a specific temperature, strain rate increases linearly with the impact velocity of striker. No obvious relationship is observed between the elastic modulus and strain rate.

(4) The peak stress and peak strain have significant rate effect before and after thermal treatment. Both of them increase with strain rate, but the gradients of increase are quite different under different temperatures. Below 500°C, the influence of temperature is slight, while it becomes significant for temperatures above 500°C.

### Acknowledgments

This work was supported by the National Natural Science Foundation of China (51379147, 51579062).

### References

Branlund, J. M., & Hofmeister, A. M. (2007). Thermal diffusivity of quartz to 1000°C: effects of impurities and the  $\alpha$ - $\beta$  phase transition. *Physics & Chemistry of Minerals*, 34(8): 581-595.



- Chong, K.P., Hoyt, P.M., Smith, J.W., et al., (1980). Effects of strain rate on oil shale fracturing. *International Journal of Rock Mechanics and Mining Science* 17(1): 35-43.
- Christensen, R.J., Swanson, S.R., Brown, W.S., (1972). Split Hopkinson-bar tests on rock under confining pressure. *Experimental Mechanics* 12(11): 508-513.
- Dai, F., Huang, S., Xia, K., et al., (2010). Some fundamental issues in dynamic compression and tension tests of rocks using split Hopkinson pressure bar. *Rock Mechanics & Rock Engineering* 43(6): 657-666.
- Du, S.J., Liu, H., Zhi, H.T., (2004). Testing study on mechanical properties of post-high-temperature granite. *Chinese Journal of Rock Mechanics and Engineering* 23(14):2359-2364. (in Chinese)
- Frew, D.J., Forrestal, M.J., Chen W (2002). Pulse shaping techniques for testing brittle materials with a split Hopkinson pressure bar. *Experimental Mechanics* 42(42): 93-106.
- Funatsu, T., Seto, M., Shimada, H., et al., (2004). Combined effects of increasing temperature and confining pressure on the fracture toughness of clay bearing rocks. *International Journal of Rock Mechanics & Mining Sciences* 41(6): 927-938.
- Jackson, K., Kingman, S.W., Whittles, D.N., et al., (2008). The effect of strain rate on the breakage behavior of rock. *Archives of Mining Sciences* 53(1): 3-22.
- Jeong, H.S., Kang, S.S., Obara, Y., (2007). Influence of surrounding environments and strain rates on the strength of rocks subjected to uniaxial compression. *International Journal of Rock Mechanics & Mining Sciences* 44(3): 321-331.
- Kolsky, H., (2002). An Investigation of the Mechanical Properties of Materials at very High Rates of Loading. *Proceedings of the Physical Society* 62(11):676.
- Liang, C.Y., Zhang, Q.B., Li, X., et al., (2015). The effect of specimen shape and strain rate on uniaxial compressive behavior of rock material. *Bulletin of Engineering Geology & the Environment*: 1-13.
- Liu, S., Xu, J.Y., (2015). An experimental study on the physic-mechanical properties of two post-high-temperature rocks. *Engineering Geology* 185(2): 63-70.
- Liu, S., Xu, J.Y., (2015). Effect of strain rate on the dynamic compressive mechanical behaviors of rock material subjected to high temperatures. *Mechanics of Materials* 82: 28-38.
- Lu, Z.T., Wang, Z.L., (2016). Triaxial tests on dynamic properties of granite under intermediate and high strain rates. *Chinese Journal of Geotechnical Engineering* 38(6): 1087-1094. (in Chinese)
- Nasseri, M.H.B., Tatone, B.S.A., Grasselli, G., et al., (2009). Fracture Toughness and Fracture Roughness Interrelationship in Thermally treated Westerly Granite. *Pure & Applied Geophysics* 166(5): 801-822.
- Ozguven, A., Ozcelik, Y., (2014). Effects of high temperature on physico-mechanical properties of Turkish natural building stones. *Engineering Geology* 183: 127-136.
- Qi, C.Z., Wang, M.Y., Qian, Q.H., (2009). Strain-rate effects on the strength and fragmentation size of rocks. *International Journal of Impact Engineering* 36(12): 1355-1364.
- Rocchi, V., Sammonds, P.R., Kilburn, C.R.J., (2002). Flow and fracture maps for basaltic rock deformation at high temperatures. *Journal of Volcanology and Geothermal Research* 120: 25-42.
- Sheinin, V.I., Blokhin, D.I., (2012). Features of thermomechanical effects in rock salt samples under uniaxial compression. *Journal of Mining Science* 48(1): 39-45.
- Wu, W., Zhang, W.D and Ma, G.W., (2010). Mechanical properties of copper slag reinforced concrete under dynamic compression. *Construction and Building Materials* 24(6): 910-917.
- Yin, T., Li, X., Xia, K., et al., (2012). Effect of thermal treatment on the dynamic fracture toughness of Laurentian granite. *Rock Mechanics & Rock Engineering* 45(6):1087-1094.
- Yuan, G., Liu, Q.S., (2011). Research for time-temperature equivalence effect of rock (II): Experimental research. *Rock and Soil Mechanics* 32(4): 961-966.

- Zhai, Y., Ma, G.W., Zhao, J.H., et al., (2007). Dynamic failure analysis on granite under uniaxial impact compressive. *Chinese Journal of Geotechnical Engineering* 29(3): 385-390. (in Chinese)
- Zhang, J., Ma, W., Zhang, F., et al., (1996). On rock structure character under high temperature. *Journal of North-eastern Univer-sity* 17(1): 5-9. (in Chinese)
- Zhou, Y.X., Xia, K., Li, X.B., et al., (2012). Suggested Methods for Determining the Dynamic Strength Parameters and Mode-I Fracture Toughness of Rock Materials. *International Journal of Rock Mechanics & Mining Sciences* 49(1): 105-112.